The Divinylborinium System and its Al, Ga, In, and Tl Congeners: Quantitative Theoretical Predictions and Qualitative Bonding Analysis

Longfei Li,[a,b] Ming Lei,[a]* Yaoming Xie,[b] Frank Weinhold,[c]
and Henry F. Schaefer III[b]*

[a] *State Key Laboratory of Chemical Resource Engineering, Institute of Materia Medica, College of Science, Beijing University of Chemical Technology, Beijing 100029, PR China*

[b] *Center for Computational Quantum Chemistry, University of Georgia, Athens, GA 30602, U. S. A.*

[c] Department of Chemistry, University of Wisconsin, Madison, Wisconsin, 53706, *U.S.A.*

*Email: ccq@uga.edu (H. F. Schaefer), leim@mail.buct.edu.cn (M. Lei)

ABSTRACT

A substituted divinylborinium cation has been synthesized recently and characterized crystallographically as a *gauche* structure with a 153° C1-C2-C3-C4 dihedral angle. A full theoretical geometrical optimization of the bis-(2-mesityl-1,2-diphenylvinyl)-borane cation shows excellent agreement with the crystal structure. However, for the parent unsubstituted divinylborinium cation, we predict a nearly 90° C1-C2-C3-C4 dihedral angle using the CCSD(T)/cc-pVTZ coupled cluster method. The *cis* and *trans* planar geometries (0° and 180° for the C1-C2-C3-C4 dihedral angle) proved to be transition states with energy barriers of 2.8 and 2.3 kcal/mol, respectively, with respect to unimolecular conversion to the *gauche* equilibrium. The much larger C1-C2-C3-C4 dihedral angle for the mesityl disubstituted divinylborinium is associated with its higher energy barrier for rotation, due to the π-π stacking effects of the outer-sphere phenyl groups. The structures of the heavier boron group cations (Al, Ga, In, and Tl) have also been investigated here, finding even lower energy barriers (0.3 ~ 0.7 kcal/mol). After the ZPVE corrections, the barriers are further decreased. The torsional angles for the unknown Al, Ga, In, and Tl dimesityl substituted compounds should be somewhat less than 153°. Many of these findings may be understood in terms of qualitative electronic structure theory. The torsional folding of borane complex, including cationic divinylborinium and elementary vinylborane ($C_2H_3BH_2$) or chlorovinylborane (C_2H_3BHCl) precursors, are investigated with natural bond orbital (NBO) analysis to unveil the electronic origins of the torsional properties. The NBO-based descriptors are employed to systematically "deconstruct" complex torsional dependence into a balanced portrayal of hyperconjugative and steric effects.

1. Introduction

There is much recent interest in the chemistry of boron cations[1-2] (borinium[3], borenium,[4-7] and boronium[8] ions; shown in Scheme 1), in part because of their strong Lewis acidity and coordinative unsaturation.[9-10] Boron cations can be relevant to catalysis and anion sensing, or serve as synthons for the organoboron materials field.[11] As the number of ligands increases, the Lewis acidity at the boron atom decreases, and the degree of the acidity is expected to follow the order: borinium > borenium > boronium.[12] In 2007, Cowley and coworkers reported the first boron dication, which is stabilized by two β-diketiminate ligands.[13]

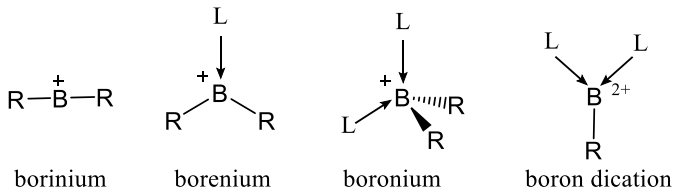

Scheme 1. Four distinct classes of boron cations; L = Lewis base.

The positively charged borinium (R-B^{+}-R), featuring two empty *p*-orbitals, deviates significantly from the octet rule.[14] As a result, borinium displays extraordinary Lewis acidity and readily forms complexes with electron-rich heteroatoms such as oxygen and nitrogen.[15-16] Due to their extreme reactivity, the borinium cations are very difficult to be synthesized. However, borinium can be stabilized by *p*-donor ligands, which are capable of n-back-bonding, so that the large positive charge at the boron center is offset and nucleophilic attack is inhibited.[17] Although two-coordinated borinium cations were detected with mass spectrometric studies very early,[18-20] the borinium ions had not isolated

until 1982. In back-to-back papers. Nöth et al. synthesized and characterized the dimidinate diamidoboron cation $(tmp{=}B{=}NR_2)^+$ (R = CH_3, C_2H_5; tmp = 2,2,6,6-tetramethylpiperidino) and the amido(organy1)boron cation $(tmp{=}B\text{-}R)^+$,[21] while Parry and coworkers synthesized and characterized the borinium ion $[(i\text{-}Pr)_2N\text{-}B^+\text{-}N(i\text{-}Pr)_2]$.[22] Subsequently, more boriniums such as the methoxy ($CH_3OB^+OCH_3$) and dimethylamino $[(CH_3)_2NB^+N(CH_3)_2]$ compounds have been observed.[23-25] The optimal orbital overlap between two empty *p* orbitals on boron and the lone-pair *p* orbitals of the two ligands will lead to a nearly linear R-B-R angle for borinium cations.[26-27] Schwarz and coworkers performed theoretical computations for the $B(OH)_2^+$ cation, and suggested that the substantial *p* stabilization results in an almost linear OBO arrangement.[28] Stephen and coworkers synthesized the $^tBu_3P{=}N\text{-}B^+\text{-}N{=}P^tBu_3$ borinium ion, also indicating a linear arrangement of the five atoms composing the $P{=}N\text{-}B^+\text{-}N{=}P$ linkage.[29] Kenttämaa *et al.* reported pioneering research on gas-phase borinium ion chemistry using a dual cell Fourier-transform ion cyclotron mass spectrometer.[30]

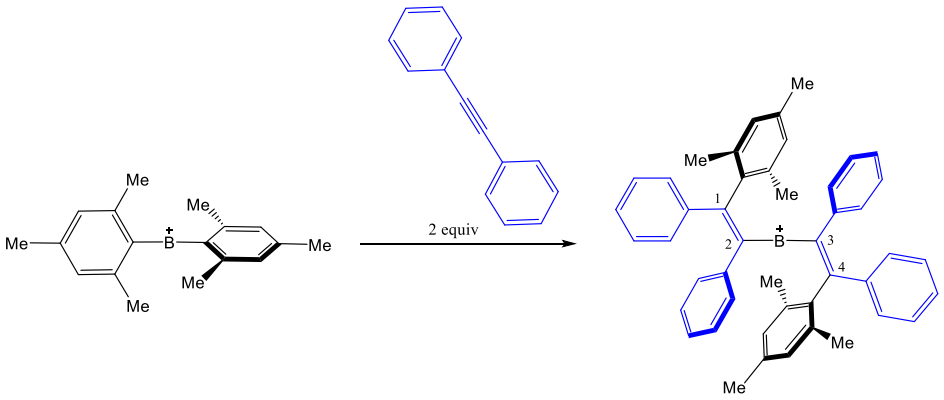

Scheme 2. The synthesis of the stable divinylborinium ion by Tanaka and coworkers.[31]

In 2014, Shoji *et al.* reported the synthesis, structure, and reactivity of the two-

coordinated boron cation, dimesitylborinium (Mes_2B^+), with linear C–B^+–C bonding,[32] and found it displays high thermal stability. In 2017, the same research group found that the Mes_2B^+ can undergo twofold 1,2-carboboration reactions with two equivalents of diphenylacetylene, and the authors synthesized the stable mesityl disubstituted divinylborinium, shown in Scheme 2.[31] Contrary to the expectation to give products with a higher coordination number for the boron atom, this substituented divinylborinium was devoid of further coordination. Similar to the simple *p*-donor ligands, this divinylborinium is suggested to be stabilized by the p-π interactions between the boron center and two vinyl substituents. Both NMR spectra and DFT computations suggest that the positive charge of the cation is delocalized over the entire conjugated system, and the electron density is transferred from the π bonds of the vinyl ligands to the boron atom. However, an unusual value of 152.8° for the C1-C2-C3-C4 dihedral angle was observed crystallographically for this divinylborinium. This structure for the stable boron-containing compound may also give insights into the unknown heavier congeners, namely Al, Ga, In, and Tl. The theoretical study of the electronic structure for the *trans, cis,* and *guache* divinylboriniums may shed the light of the nature of the chemical bonds for the boron cations. In the present research, we will study the divinylborinium, $B(C_2H_3)_2$, as well as its analogs $M(C_2H_3)_2$, (M = Al, Ga, In, Tl).

2. Computational Methods

Coupled-cluster theory with single and double excitations augmented by a perturbative treatment of triple excitations CCSD(T) was applied to the unsubstituted divinylborinium with CFOUR.[33] All geometrical parameters were optimized with the CCSD(T) method.

The initial geometries are from the experimental results if available, and those for the simple models are built by chemical intuition. DFT (ωB97X-D[34] functional) computations were also performed with Gaussian09.[35] The cc-pVTZ basis sets were used for all atoms except In and Tl, for which the relativistic effective core potential cc-pVTZ-PP basis sets were used. The harmonic vibrational frequencies of all optimized structures are used to verify these systems to be either genuine minima or transition states (first-order saddle points). All optimized geometries can be found in the Cartesian.xyz file, available in the supplementary information. NBO analyses were carried out to explain the torsional angles, based on hyperconjugative and steric effects.[36]

3. Results and Discussion

A. Two Compounds Synthesized by Tanaka and Coworkers.

Two important crystal structures (cation and neutral molecule) were determined by Tanaka, Shoji, Hashizume, Sugimoto, and Fukushima.[31] Both compounds are too large (at this time) to be fully optimized structurally with the CCSD(T) method using a good basis set. Therefore, in Figure 1, we report the ωB97X-D (cc-pVTZ) optimization of the neutral chloro-bis-(2-mesityl-1,2-diphenylvinyl)-borane. Our theoretical structure is there compared to the Tanaka crystal structure in Figure 1.

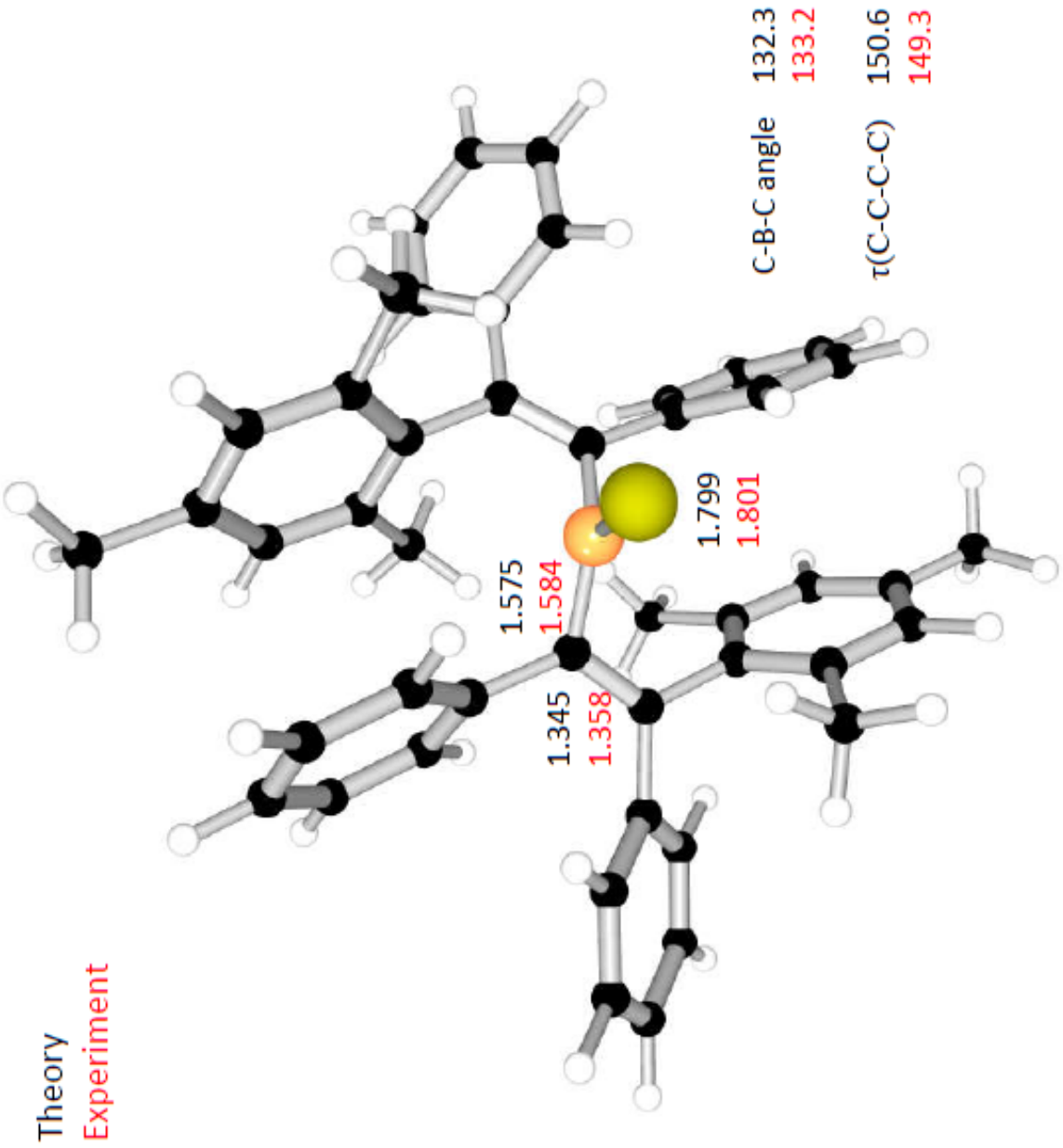

Figure 1. Theoretical and experimental structures for neutral chloro-bis-(2-mesityl-1,2-diphenylvinyl)-borane. Bond distances are in Å. All structural features of freedom have been fully optimized. See SI for details.

The agreement between ωB97X-D/cc-pVTZ geometry and the crystal structure is excellent. All the theoretical bond distances are shorter than those observed in the lab. The central B-C distance is 1.575 for theory *vs* 1.584 Å for experiment. The C-C distance close to the B atom is 1.345 (theory) or 1.358 (crystal structure). The variance with the theoretical structure is the B-Cl distance, with theory predicts 1.799, 0.002 Å less than the experimental value of 1.801 Å for the B-Cl distances. The central C-B-C bond angle is 132.3° from theory and 133.2° in the crystal structure.

The most important result of the Tanaka research was the successful synthesis and structure determination of the cation bis-(2-mesity-1,2-diphenylvinyl)-borane. The actual experimental crystal structure includes the counteranion boron cluster $[HCB_{11}Cl_{11}]^-$. The crystal structure also includes an ortho-dichorobenzene (ODCB) connected via an intermolecular CH---Cl interaction.

In Figure 2 is reported a theoretical equilibrium geometry, along with the experimental crystal structure. The theoretical cation structure (Figure 2) shows very good agreement with experiment. This is so even though the cation structure includes the boron cluster anion $[HCB_{11}Cl_{11}]^-$ and the hydrogen bonded ODCB. The largest difference between theoretical and experimental bond distance is 0.01 Å, for the central B-C distances. The central C-B-C bond angle is (170.5°, theory) or 168.5° (experiment). The theoretical CCCC dihedral angle (149.3°) is 3.5° less than that found in the crystal structure. In what follows, we will see that this dihedral angle is very different from that predicted for the parent divinyl borinium cation.

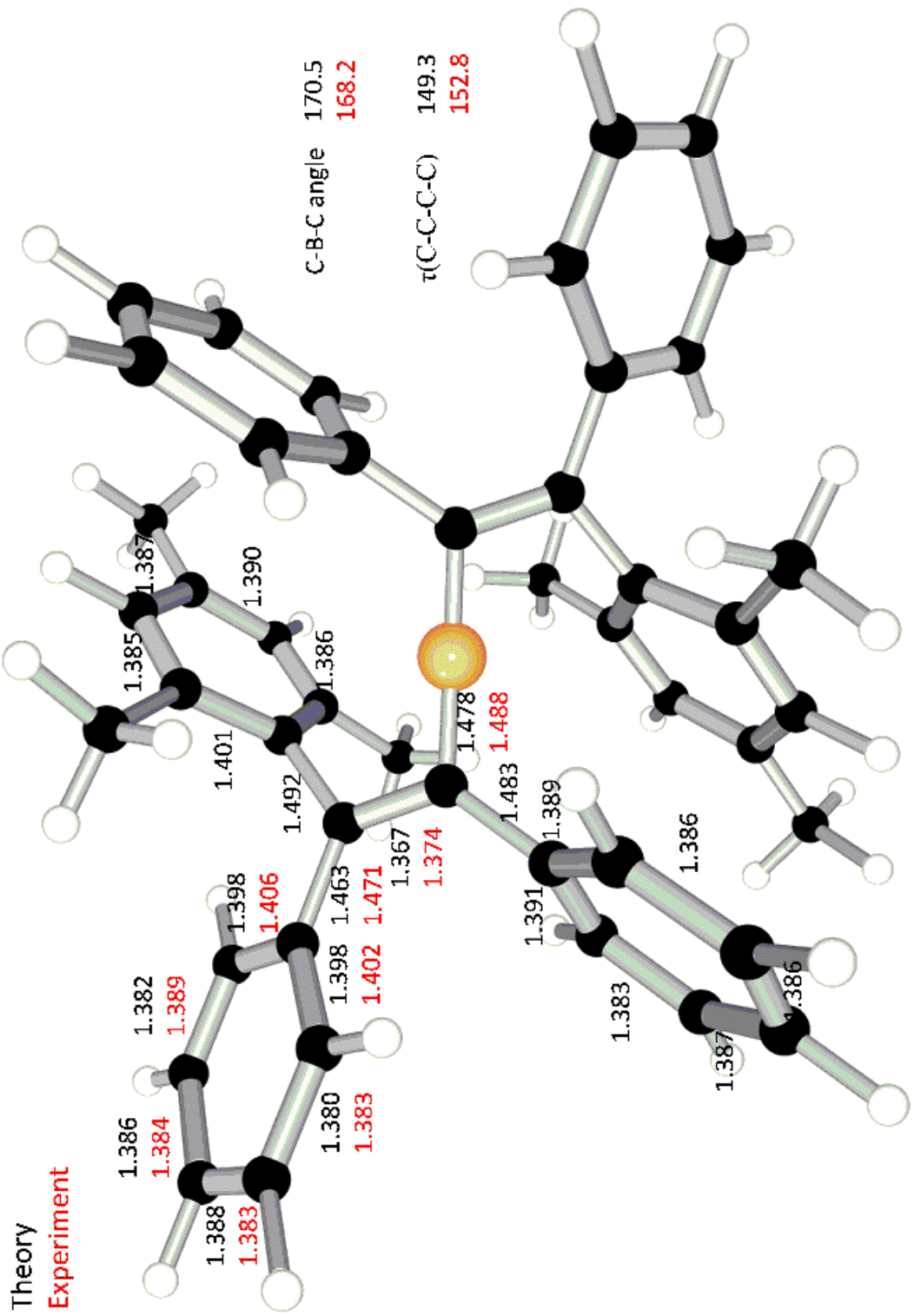

Figure 2. The bis-(2-mesity-1,2-diphenylvinyl)-borane cation structure, from theory (black) and experiment (red). All structural featurs have been fully optimized. See SI for detail.

B. The Unsubstituted Divinylborinium Cation

The global minimum and the symmetry-constrained transition states for the unsubstituted divinylborinium were studied at the CCSD(T)/cc-pVTZ level. The optimized stationary point geometries are shown in Figure 3. The global minimum is a *gauche* structure with C_2 symmetry. The C2-B-C3 angle is predicted to be 177°, and the C1-C2-C3-C4 dihedral angle is predicted to be 89°. The two planar structures (*cis* and *trans*) for the unsubstituted divinylborinium proved to be transition states, each with one imaginary vibrational frequency. Examining the corresponding normal modes, we confirm that both the *cis* and *trans* transition states are connected to the *gauche* minimum.

The energies of the *cis* and *trans* divinylborinium cation transition states are higher than the *gauche* structure, namely by 2.8 (*cis*) and 2.4 (*trans*) kcal/mol, respectively. It is easily understood that the *gauche* structure is lower in energy due to the p-π conjugate effect involving the two perpendicular p orbitals of the boron center, each interacting with the π orbital of a vinyl group. In contrast, the *cis* (or *trans*) transition state has a single π-p-π conjugate system involving only one p orbital of the boron center, interacting with the π orbital of two vinyl groups. In other words, for the planar (*cis* or *trans*) transition states, the in-plane p orbital of the boron atom is not involved in the conjugated system.

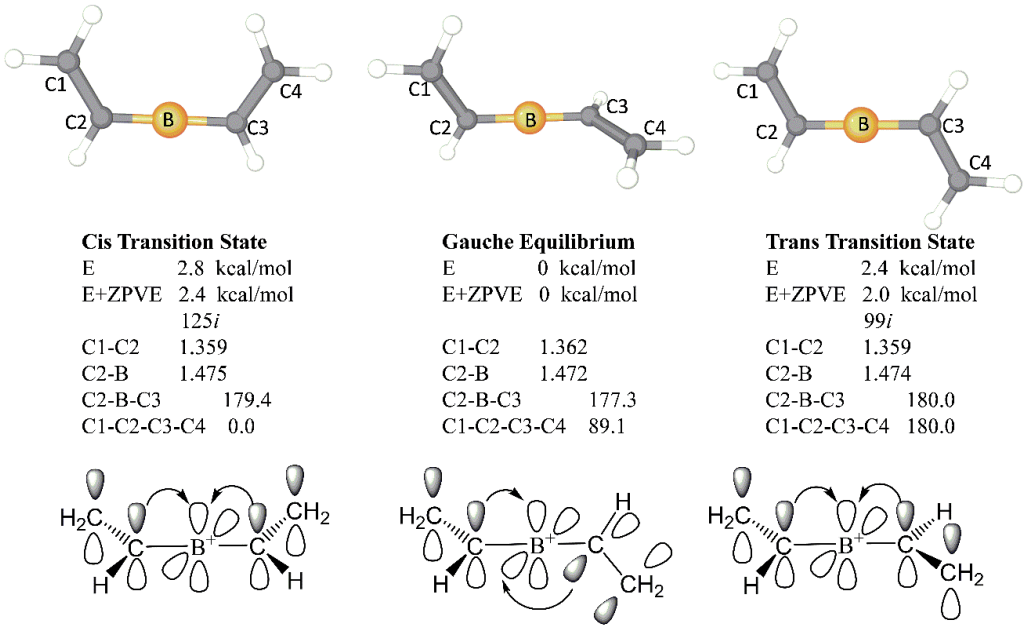

Figure 3. Coupled cluster CCSD(T)/cc-pVTZ structures and the relative energies (with and without ZPVE corrections) for the unsubstituted divinylborinium ion including the *trans* transition state, *gauche* equilibrium and *cis* transition state. The bond lengths are in Å.

Let us now return to the X-ray crystal structure of the bis-(2-mesityl-1,2-diphenylvinyl)-borane cation[31]. That experimental structure shows 1.488 Å for the C2-B length, 1.374 Å for the C1-C2 length, 168.2° for the C2-B-C3 angle, and 152.8° for the C1-C2-C3-C4 dihedral angle. The CCSD(T) central bond distances are in good agreement with experiment.

The lower level ωB97X-D distances are 0.030 Å (C1-C2) and 0.022 Å (C2-B) away from the experiment for the synthesized compound. Before going further, we emphasize the broad agreement of the ωB97X-D structure with that predicted by the more reliable CCSD(T) method.

The theoretical dihedral angle 89.1° for the parent divinyl structure is very different from the 152.8° found for the experimental structure (Figure 2). How should we respond to this striking difference? As reported above, when the full bis-(2-mesityl-1,2-

diphenylvinyl)-borane cation is optimized, there is good agreement between theory and experiment. It must first be noted that the energy barrier for the rotation of the unsubstituted divinylborinium (the parent) is only 2.4 ~ 2.8 kcal/mol. Therefore, the equilibrim torsional angle may be largely influenced by the steric or static effects between the substituents of vinyl groups. The experimental vs. CCSD(T) bond distances are (1.488 - 1.372) = 0.016Å for C2-B and (1.374 – 1.362) = 0.012 Å for C1-C2.

C. The Al, Ga, In, and Tl Analogs.

The heavier group-13 element (Al, Ga, In, and Tl) congeners were also studied at the ωB97X-D/cc-pVTZ level. We obtain generally analogous results. As shown in Figure 4, the planar structures are transition states with 0° (*cis*) or 180° (*trans*) dihedral angles, while the *gauche* structures are minima with C1-C2-C3-C4 dihedral angles near 90°. The energy barriers of transition states with respect to the minima for the Al, Ga, In, and Tl system are 0.3-0.6 kcal/mol for the *cis* transition state or 0.4-0.7 kcal/mol for the *trans* transition state. These barriers are much lower than that for the unsubstituted divinylborinium (entry 1 in Table 1). This is due to the weaker conjugate effects between the empty p orbtials of the Al, Ga, In, or Tl center and the π orbitals of the vinyl groups, compared with situation for the boron case. After the ZPVE corrections, the energy barriers for the transition states become even lower and close to zero. In reality, the vinyl groups can rotate freely around the C-M^+-C (M = Al, Ga, In, Tl) bond because of these low energy barriers.

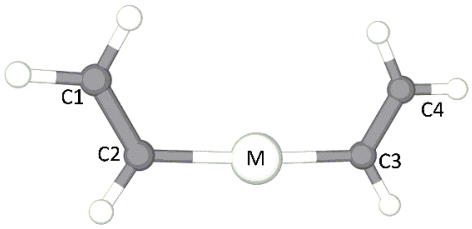

Cis Transition State

	C1-C2	C2-M	C2-M-C3	C1-C2-C3-C4
B	1.344	1.466	180.0	0.0
Al	1.336	1.891	176.6	0.0
Ga	1.332	1.892	178.2	0.0
In	1.329	2.074	178.7	0.0
Tl	1.325	2.099	179.2	0.0

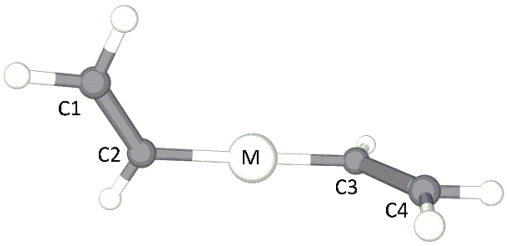

Gauche Equilibrium

	C1-C2	C2-M	C2-M-C3	C1-C2-C3-C4
B	1.347	1.464	178.0	85.8
Al	1.337	1.890	177.1	84.7
Ga	1.333	1.890	178.5	85.2
In	1.329	2.073	178.5	101.1
Tl	1.325	2.097	179.5	85.8

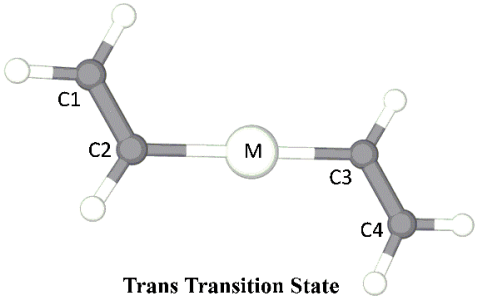

Trans Transition State

	C1-C2	C2-M	C2-M-C3	C1-C2-C3-C4
B	1.345	1.465	180.0	180.0
Al	1.336	1.890	180.0	180.0
Ga	1.332	1.892	180.0	180.0
In	1.328	2.074	180.0	180.0
Tl	1.325	2.098	180.0	180.0

Figure 4. Structures for the unsubstituted divinylborinium and its heavier congeners, computed with the ωB97X-D/cc-pVTZ method. M represents B, Al, Ga, In, or Tl. The bond lengths are in Å.

Table 1. Relative energies (kcal/mol; computed with the ωB97X-D method) of the boron group-element unsubstituted divinyl ion for the c*is* transition states, *gauche* equilibria and *trans* transition states. The cc-pVTZ basis sets are used for all the atoms, except In and Tl, for which cc-pVTZ-PP basis sets are used.

	Cis Transition		Gauche Equilibrium		*Trans* Transition	
	E	E+ZPVE	E	E+ZPVE	E	E+ZPVE
B	2.5	1.9	0.0	0.0	2.1	1.4
Al	0.6	0.2	0.0	0.0	0.5	0.1
Ga	0.7	0.3	0.0	0.0	0.6	0.1
In	0.4	0.1	0.0	0.0	0.4	-0.1
Tl	0.4	-0.1	0.0	0.0	0.3	-0.2

D. NBO Analysis of Torsional Folding

Molecular shapes are thought often to be primarily dictated by the "folding" propensities associated with low-frequency torsional modes of vibration. These torsional properties, like those of bending and stretching modes, are dictated by the electronic interactions of the chemical bonding network that underlies the Born-Oppenheimer potential energy surface (PES). The chemical bond network in turn requires the quantum-mechanical imagery of orbital interactions for visualization purposes. In the present section we employ natural bond orbital (NBO) analysis[36] to investigate the electronic origins of the torsional properties of the divinylborinium system in terms of familiar orbital-type chemical conceptions.

From the 1930s onward, theoretical studies of torsional phenomena focused primarily on the rotation barriers of ethane and related saturated hydrocarbon chains. These studies led to ongoing controversies[37] over the relative importance of contributions from interactions of steric vs. hyperconjugative type[38] (also known as "donor-acceptor",[39] "stereoelectronic",[40] or "resonance-type" [41] interactions). Although the latter viewpoint has

gained significant support in current research[42] and teaching,[43] opposing viewpoints (predictably based on the ambiguities of nonorthogonal orbital analysis) continue to appear in the chemical literature.[44] Critical consideration of these issues for torsional features of a novel Group-13 compound therefore allows fresh assessment of the interpretive and predictive utility of the hyperconjugative picture of rotation barriers in a catalytically important species.

The "hypovalent" character of boron (and heavier Group-13 congeners) is well known to be associated with the formally empty valence-*p* orbital, labelled "lone vacancy" (LV) in NBO output, or symbolized as "p_B*" for present purposes. Such a low-lying p_B* "hole" in the atomic valence-electron configuration can be recognized as a powerful electronic acceptor (Lewis acid) site, with hyperconjugative interactions that are markedly stronger than those of the σ_{CH}* (2-center CH antibond) acceptor orbitals of ethane barriers. As usual, the simple hyperconjugative propensities of a carborane backbone chain may be opposed by steric clashes of filled orbitals in attached pendant groups to yield a more complex torsional profile. However, the availability of NBO descriptors for both hyperconjugative (donor-acceptor) and steric (donor-donor) interactions allows such competing effects to be disentangled and quantified. For present purposes we employ the simple B3LYP/LANL2DZ-level description that can be readily extended to heavier Group 13 homologs, allows practical $DEL-deletion re-optimizations (as described below), and agrees satisfactorily with higher-level methods both for smaller skeletal backbone models and fully substituted derivatives.

In the present case, we first consider the NBOs of the elementary vinylborane ($C_2H_3BH_2$) or chlorovinylborane (C_2H_3BHCl) precursors to the divinyl and higher derivative species.

Figure 5 displays pNBO[45] overlap visualizations for the dominant π_{CC}-p_B* interaction of $C_2H_3BH_2$ (left) and C_2H_3BHCl (right), showing the hyperconjugative preference for a planar equilibrium geometry (φ_{CCBH} = 0 or 180) in each case.[46]

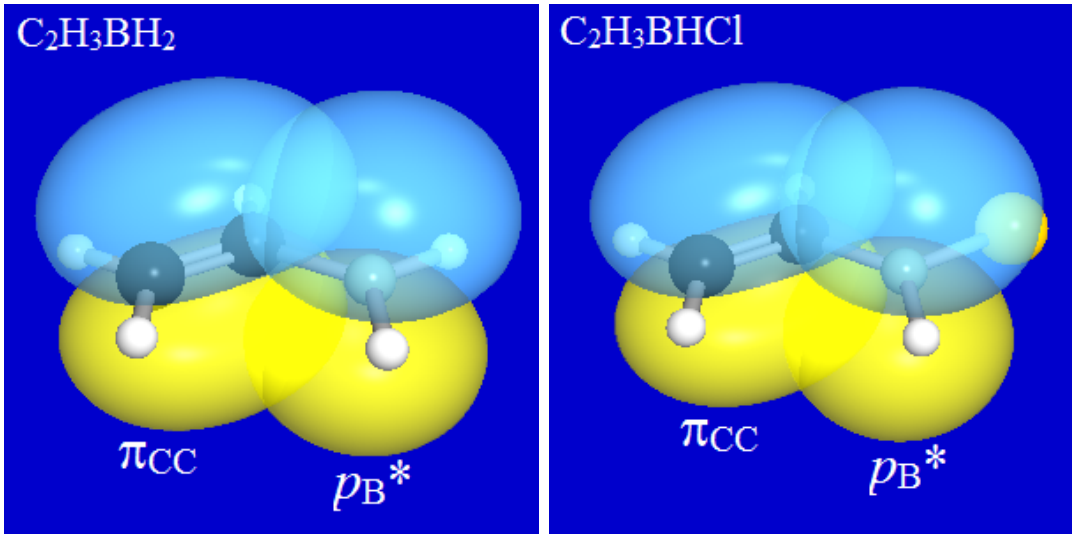

Figure 5. pNBO overlap diagrams for donor-acceptor π_{CC}-p_B* interactions in $C_2H_3BH_2$ (left) and C_2H_3BHCl (right), showing the strong resemblance of hyperconjugative interactions favoring planar equilibrium geometry (φ_{CCBH} = 0 or 180) in each case.

Figure 6 presents relaxed torsional scans for a variety of precursor species relevant to the present study. The top two curves of Figure 6 display the full φ_{CCBH} torsional dependence for the monovinyl $C_2H_3BH_2$ (circles) and C_2H_3BHCl (triangles) shown in Figure 5. Both torsional curves exhibit the expected high barrier (ca. 8 kcal/mol) at orthogonal φ_{CCBH} = 90 geometry, where the powerful π_{CC}-p_B* donor-acceptor interaction vanishes by symmetry (only partially compensated by hyperconjugation with the weaker σ_{CC}, σ_{CH} donors that swing into alignment with p_B* at other angles). Except for a secondary well and barrier that develop near the *cis* limit (see below), a similar preference for planarity is shown in the corresponding curve for the *trans*-like divinyl derivative $BCl(C_2H_3)_2$ (squares), where the anti-cooperative effects of serving multiple donors ("busy

p_B* acceptor orbital") appreciably weaken the barrier. Nevertheless, the tendency of leading adjacent π_{CC} donor orbitals to co-align with the dominant p_B* acceptor orbital is evident in all these species.

For the unusual cusp-like behavior of $BCl(C_2H_3)_2$ in Figure 6, it is fairly clear that it represents a genuine excited-state curve-crossing, rather than the usual "strongly avoided crossing" on the ground-state PES (in a Marcus-like picture). This unusual mixing of "non-covalent" conformational change with electronic excitation indicates the "non-innocent" character of torsional transition in this species, through strong coupling to low-lying conical intersections and related changes of covalent bonding pattern. Full analysis of this cusp-like region would require investigation of corresponding excited-state properties. However, the evident connection to electronic rearrangements suggests how conformational control may serve as an important electronic "switch" for catalytic activity of these species.

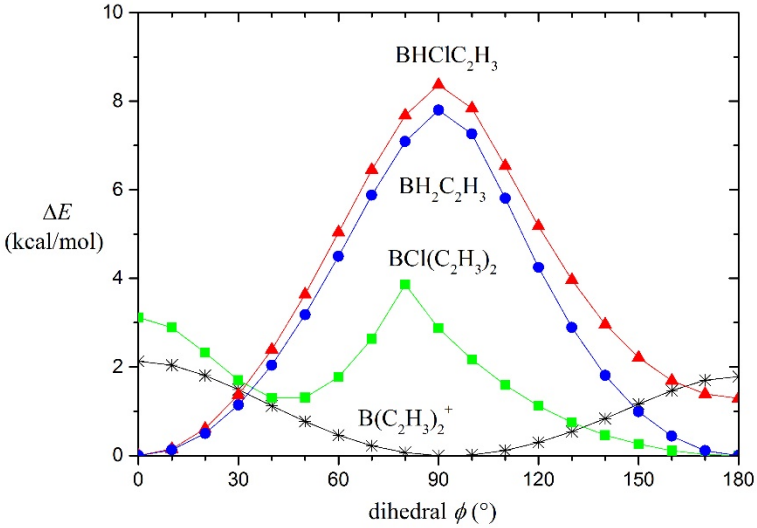

Figure 6. $\Delta E(\varphi)$ relaxed torsional scans for $B(C_2H_3)_2^+$ (φ_{CCCC}; star signs), $BCl(C_2H_3)_2$ (φ_{CCBCl}; squares), $BH_2C_2H_3$ (φ_{CCBH}; circles), and $BHClC_2H_3$ (φ_{CCBH}; triangles), B3LYP/LANL2DZ level.

How can we be certain that the π_{CC}-p_B* donor-acceptor interaction of Figure 5 is indeed the authentic "cause" of the torsional "effects" in Figure 6? Unique cause-effect specificity can be established with NBO deletion ($DEL keylist) techniques[47] that allow one to *delete* one or more donor-acceptor interactions from the full calculation and recalculate the PES (and associated structural, vibrational and reactive properties) as if such interactions were absent in nature. Such variational $DEL reoptimization techniques require interactive interfacing between a host electronic structure system (such as GAMESS or Gaussian) and the NBO program, involving single-pass energy evaluation (by the host program) of a perturbed density (provided by the NBO program) that formally "undoes" the density shift of a specified NBO donor-acceptor interaction, without requiring 4-index integral transformations. Although such $DEL type re-optimizations and frequency calculations are numerically tedious (because the necessary gradient and Hessian derivatives are evaluated numerically rather than analytically), they provide a powerful analysis tool for relating specific structural features of interest to specific donor-acceptor interactions. The qualitative hyperconjugative origin of a structural perturbation generally becomes clear at lower levels than are required to achieve a desired degree of quantitative accuracy.

Figure 7 depicts the reoptimized geometries and torsional φ_{CCCC} angles for deletion of one (central panel) or both (right panel) π_{CC}-p_B* donor-acceptor interactions of $BCl(C_2H_3)_2$, compared with the full computation (left panel). As shown in the panels, the vinyl appendages along the BCl body axis can be made to "flap like a bird" between planar and non-planar conformations depending on which π_{CC}-p_B* interactions are retained or deleted. It is remarkable that the small stabilization energy associated with the key π_{CC}-p_B*

hyperconjugation in $C_2H_3BH_2$ (estimated as 25.5 kcal/mol by 2nd-order perturbation theory, or 28.0 kcal/mol by $DEL deletion) is only about 0.04% of total electronic energy, yet able to exert *qualitative* influence on overall molecular shape and other properties. Similar $DEL-type deletion searches can generally be used to identify the hyperconjugative "smoking gun" responsible for a specific structural, vibrational, or reactive property of interest.

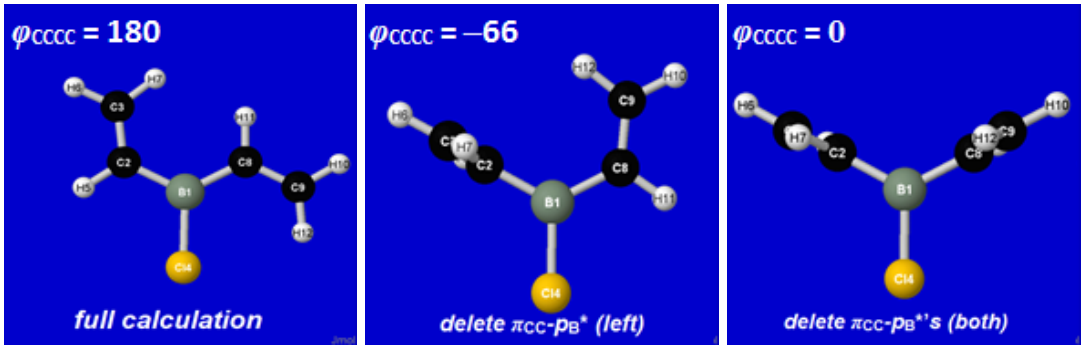

Figure 7. Dependence of optimized $BCl(C_2H_3)_2$ torsional φ_{CCCC} angles on $DEL-type deletions of zero (left), one (center), or both π_{CC}-p_B* donor-acceptor interactions.

In the context of strong π_{CC}-p_B* hyperconjugative forces, it is also quite interesting to examine the corresponding torsional barriers of the monovinyl ($C_2H_3BH^+$) or divinyl ($C_2H_3BC_2H_3^+$) borinium cations, where *two* orthogonally oriented lone vacancies p_B*, $p^{\perp}_B$* are available at the boron center. In these cases, it is easy to see that if the linkages to boron (viz., C-B-H in $C_2H_3BH^+$ or C-B-C in $C_2H_3BC_2H_3^+$) become *linear*, then the sum of π_{CC}-p_B* and π_{CC}- $p^{\perp}_B$* interactions must be *constant*, resulting in *no* net torsional force at any φ. Indeed, the C-B-H bending angle is found to be *always* linear in $C_2H_3BH^+$, while the corresponding C-B-C angle of $C_2H_3BC_2H_3^+$ is slightly bent only in the near-*cis* region of weak vinyl-vinyl steric clash (see below). It is seen as a consequence (Figure 6) that

$C_2H_3BH^+$ presents no rotation barrier, while that of $C_2H_3BC_2H_3^+$ is non-zero in the near-*cis* and near-trans regions where the contributions of π_{CC}-p_B* and π_{CC}- $p^{\perp}_B$* interactions are not perfectly cancelling. Thus, even the weak or non-existent rotation barriers in the cationic borinium derivatives reflect the important consequences of strong π_{CC}-p_B* hyperconjugations in partially exposed vs. cancelling combinations.

As alluded to above, steric influences are also present whose effects can be quantified with the NBO-based STERIC keyword analysis [48]. In the case of $BCl(C_2H_3)_2$, the torsional potential of Figure 6 (squares) exhibits an interesting asymmetry in planar *cis* and *trans* geometries. The global minimum lies at the *trans* (φ_{CCCC} = 180°) limit, but a slightly twisted secondary minimum and weak barrier at the *cis*-planar limit (with no apparent explanation in terms of the hyperconjugative π_{CC}-p_B* interaction of Figure 5). In this case we can employ natural steric analysis to evaluate the pairwise estimate of steric exchange energy, $\Delta E_{\sigma\sigma'}^{(PW)}$, for each donor-donor ($\sigma\sigma'$) interaction of the bonding skeleton. Figure 8 displays the dihedral dependence $\Delta E_{\sigma\sigma'}^{(PW)}(\varphi)$ for the specific $\sigma_{C(3)H(7)}$ and $\sigma_{C(9)H(12)}$ NBOs that are each *cis* to an adjacent σ_{BC} linkage and hence proximal to one another in near-*cis* geometry (see figure inset). The figure shows that $\Delta E_{\sigma\sigma'}^{(PW)}(\varphi)$ rises repulsively for these two specific CH bonds as the vinyl groups approach *cis*-coplanarity (as a physical organic chemist would anticipate), whereas no similar steric clash arises in the *trans* limit. As seen in Figure 8, the proximal σ_{CH}-σ'_{CH} steric repulsion $\Delta E_{\sigma\sigma'}^{(PW)}(\varphi)$ exceeds the steric-free (hyperconjugatively dominated) near-*trans* $\Delta E(180–\varphi)$ behavior of Figure 6 for values smaller than $\varphi \approx 30°$, leading to a weak minimum and terminal barrier in the *cis*-planar limit. This weak *cis*-barrier could indeed be argued to have steric origins, but might as well be considered "the exception that proves the rule" in a broader view of torsional forces.

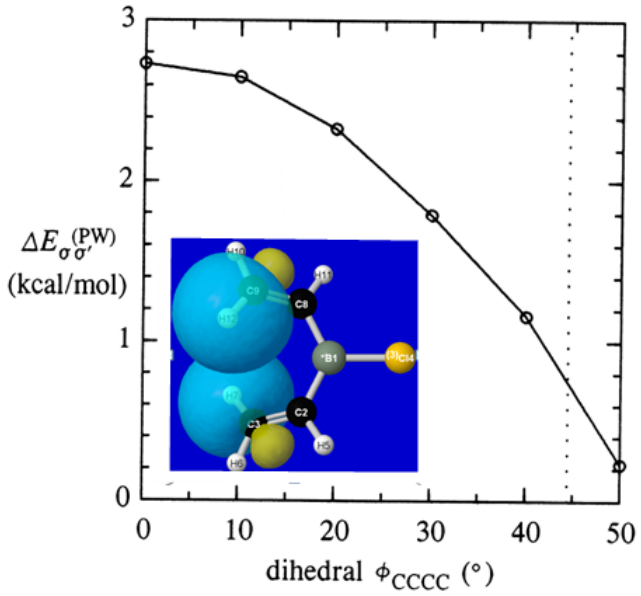

Figure 8. Torsional dependence of pairwise steric exchange energy $\Delta E_{\sigma\sigma'}^{(PW)}$ for proximal $\sigma_{C(3)H(7)}$-$\sigma_{C(9)H(12)}$ interaction in $BCl(C_2H_3)_2$. The vertical dotted line marks the near-*cis* secondary minimum (inset) at $\varphi_{CCCC} = 44°$.

Finally, we turn to the fully substituted pheny/mesityl derivatives, where steric clashes between bulky pendant groups can overcome the intrinsic torsional propensities of the unsubstituted backbone. For the $BCl(C_2H_3)_2$ backbone, Figure 6 suggests the intrinsic propensity for either *cis*-like or *trans*-like rotamers, but with likely distortions from ideal backbone angles due to steric clashes between bulky mesityl groups on the two vinyl moieties. Computations confirm the existence of two distinct torsional minima, one near $\varphi_{CCCC} = 79°$ and the other near $\varphi_{CCCC} = 152°$, but only the latter is found in the experimental crystal structure (presumably reflecting details of the synthetic procedure). As noted above, computed and experimental structural features are in excellent agreement.

To identify points of steric congestion, we again employ natural steric analysis to search for $\Delta E_{\sigma\sigma'}^{(PW)}$ values involving unfavorable σ-σ' steric contacts between filled NBOs on opposite vinyl substituents. Figure 9 displays NBO surface plots for the σ_{CH} and π_{CC}

bonds of one mesityl group that come into a 3-way "traffic jam" with a methyl σ_{CH} bond of the opposite mesityl group. The summed $\Delta E_{\sigma\sigma'}^{(PW)}$ steric repulsion values (ca. 1.6 kcal/mol; left and center panels) appear more than adequate to oppose further opening toward the *trans* geometry that is hyperconjugatively favored by less than 1 kcal/mol for $\varphi_{CCCC} \gtrsim 130°$ in the $BCl(C_2H_3)_2$ backbone (Figure 6). Consistent with such estimates from backbone species, the $E^{(2)}$ value for each hyperconjugative π_{CC}-p_B* interaction is found to fall below print threshold (< 0.5 kcal/mol) in the fully substituted derivative (Fig. 10) Thus, the physical picture is that steric repulsions of large pendant groups effectively "pin" the dihedral φ_{CCCC} angle at such a large value as to quench π_{CC}-p_B* hyperconjugation and leave the powerful p_B* Lewis acid site exposed to interaction with incoming nucleophiles.

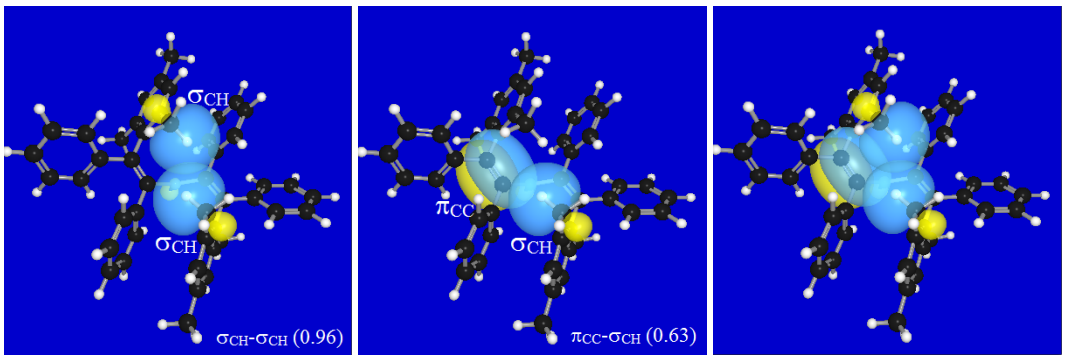

Figure 9. Steric opposition to C=C-(BCl)-C=C divinyl twisting, showing σ_{CH}-σ_{CH} (left panel), σ_{CH}-π_{CC} (middle panel), and composite (right panel) views of a methyl σ_{CH} bond of one mesityl substituent in "triangulated traffic jam" with the methyl σ_{CH} and vinyl π_{CC} bonds of the other [with individual $\Delta E_{\sigma\sigma'}^{(PW)}$ values (kcal/mol) in parentheses].

The unique C=C-B(Cl)-C=C backbone motif provides instructive examples of the complex interplay between backbone and pendant group interactions that often contribute to torsional properties. The example also illustrates how NBO-based descriptors can be employed to systematically "deconstruct" complex torsional dependence into a balanced

portrayal of hyperconjugative and steric effects, each understandable in terms of elementary bonding concepts.

Conclusions

A theoretical study of the divinylborinium cation and its heavier congeners is reported in this research. The ground-state equilibrium and two transition states of the unsubstituted divinylborinium cation are examined with coupled-cluster theory, namely CCSD(T) using the cc-pVTZ basis set. The equilibrium prefers a *gauche* structure because of stabilization from the double p-π conjugate effect between two vinyl groups and the boron center. The *cis* or *trans* transition state prefers planar structures, for which less stabilization from the π-p-π conjugate effect exists. The structures of the heavier boron group-element cations (Al, Ga, In, and Tl) have also been studied, with even lower energy barriers for the torsional rotation. In general, the energy barriers for the four heavier systems are so low as to allow the two vinyl ligands to rotate freely around the C-M-C axis. In addition, the geometries of the mesityl disubstituented divinylborinium cation is determined by the effects of the bulky substituents. We suspect that when the analogous dimesityl substituted Al, Ga, In, and Tl structures are determined experimentally they will have C-C-C-C torsion angles a bit less than 153°, due to the longer M-C distances.

Many of the above findings have been explained here using natural bond orbital concepts. The torsional folding of borane complex including cationic divinylborinium, and elementary vinylborane ($C_2H_3BH_2$) or chlorovinylborane (C_2H_3BHCl) precursors are investigated with natural bond orbital (NBO) analysis to unveil the electronic origins of torsional properties. The π_{CC}-p_B* donor-acceptor interaction is suggested to be the most probable cause of the torsional "effects". For the divinylborinium cation, the linkages to

boron become *linear*, and the sum of π_{CC}-p_B* and π_{CC}- $p^{\perp}_B$* interactions become *constant*, resulting in *no* net torsional force at any φ. The torsional force of $C_2H_3BC_2H_3^+$ is non-zero only in the near-*cis* region where the contributions of π_{CC}-p_B* and π_{CC}-$p^{\perp}_B$* interactions are not perfectly cancelling. Thus, even the weak or non-existent rotation barriers in the cationic borinium derivatives reflect the important consequences of strong π_{CC}-p_B* hyperconjugations in partially exposed vs. cancelling combinations.

Supporting Information

Cartesian coordinates of all stationary points and transition states. This material is available free of charge via the Internet at http://pubs.acs.org.

ACKNOWLEDGMENTS

The research at the Center for Computational Quantum Chemistry was supported by the U.S. National Science Foundation, Grant CHE-1661604. This work was also supported by the National Natural Science Foundation of China (Grant No. 21672018, 2161101308, and 21373023), the Beijing Municipal Natural Science Foundation (Grant No. 2162029), the Fundamental Research Funds for the Central Universities of China (Grant No. PYCC1708), and the China Scholarship Council (No. 201606880007). We thank the Special Program for Applied Research on Super Computation of the NSFC-Guangdong Joint Fund (second phase) for providing some of the computational resources.

Competing Interests

The authors declare that they have no competing interests.

REFERENCES

1. Koelle, P.; Noeth, H. The chemistry of borinium and borenium ions. *Chem. Rev.* **1985**, *85*, 399-418.
2. De Vries, T. S.; Prokofjevs, A.; Vedejs, E. Cationic tricoordinate boron intermediates: borenium chemistry from the organic perspective. *Chem. Rev.* **2012**, *112*, 4246-82.
3. Zheng, X. B.; Tao, W. A.; Cooks, R. G. Gas-phase S(N)2 reactivity of dicoordinated borinium cations using pentaquadrupole mass spectrometry. *J. Am. Soc. Mass. Spectrom.* **2001**, *12*, 948-955.
4. Prokofjevs, A.; Boussonniere, A.; Li, L.; Bonin, H.; Lacote, E.; Curran, D. P.; Vedejs, E. Borenium ion catalyzed hydroboration of alkenes with N-heterocyclic carbene-boranes. *J. Am. Chem. Soc.* **2012**, *134*, 12281-8.
5. Prokofjevs, A.; Kampf, J. W.; Solovyev, A.; Curran, D. P.; Vedejs, E. Weakly stabilized primary borenium cations and their dicationic dimers. *J. Am. Chem. Soc.* **2013**, *135*, 15686-9.
6. Stahl, T.; Muther, K.; Ohki, Y.; Tatsumi, K.; Oestreich, M. Catalytic generation of borenium ions by cooperative B-H bond activation: the elusive direct electrophilic borylation of nitrogen heterocycles with pinacolborane. *J. Am. Chem. Soc.* **2013**, *135*, 10978-81.
7. Abdalla, J. A. B.; Tirfoin, R. C.; Niu, H.; Aldridge, S. A zwitterionic hydrocarbon-soluble borenium ion based on a beta-diketiminate backbone. *Chem. Commun.* **2017**, *53*, 5981-5984.
8. Prokofjevs, A.; Kampf, J. W.; Vedejs, E. A boronium ion with exceptional electrophilicity. *Angew. Chem. Int. Ed.* **2011**, *50*, 2098-101.
9. Ramos, L. E.; Cardoso, A. M.; Correia, A. J. F.; Nibbering, N. N. M. Behaviour of arylalkylamines toward trimethyl borate as a gas-phase reagent. *Int. J. Mass spectrom.* **2000**, *203*, 101-110.
10. Shoji, Y.; Tanaka, N.; Muranaka, S.; Shigeno, N.; Sugiyama, H.; Takenouchi, K.; Hajjaj, F.; Fukushima, T. Boron-mediated sequential alkyne insertion and C-C coupling reactions affording extended pi-conjugated molecules. *Nat. Commun.* **2016**, *7*, 12704.
11. Bonnier, C.; Piers, W. E.; Parvez, M.; Sorensen, T. S. Borenium cations derived from BODIPY dyes. *Chem. Commun.* **2008**, 4593-5.
12. Jaiswal, K.; Prashanth, B.; Singh, S. Fine-Tuning of Lewis Acidity: The Case of Borenium Hydride Complexes Derived from Bis(phosphinimino)amide Boron Precursors. *Chem. Eur. J.* **2016**, *22*, 11035-41.
13. Vidovic, D.; Findlater, M.; Cowley, A. H. A beta-diketiminate-supported boron dication. *J. Am. Chem. Soc.* **2007**, *129*, 8436-7.
14. Tao, W. A.; Zheng, X. B.; Cooks, R. G. Synthesis of B, N, O-containing heterocycles via reaction of an aminoborinium ion with cyclic acetals and ketals. *J. Mass Spectrom.* **2000**, *35*, 1215-1221.
15. Wang, F.; Tao, W. A.; Gozzo, F. C.; Eberlin, M. N.; Cooks, R. G. Synthesis of B- and P-Heterocycles by Reaction of Cyclic Acetals and Ketals with Borinium and Phosphonium Ions. *J. Org. Chem.* **1999**, *64*, 3213-3223.
16. Kempen, E. C.; Brodbelt, J. Use of trimethyl borate as a chemical ionization reagent for the analysis of biologically active molecules. *J. Mass Spectrom.* **1997**, *32*, 846-854.
17. Piers, W. E.; Bourke, S. C.; Conroy, K. D. Borinium, borenium, and boronium ions:

synthesis, reactivity, and applications. *Angew. Chem. Int. Ed.* **2005**, *44*, 5016-36.
18. Dibeler, V. H.; Mohler, F. L. The Dissociation of Diborane by Electron Impact. *J. Am. Chem. Soc.* **1948**, *70*, 987-989.
19. Osberghaus, O. Die Isotopenhäufigkeit des Bors. Massenspektrometrische Untersuchung der Elektronenstoßprodukte von BF3 und BCl3. *Zeitschrift für Physik* **1950**, *128*, 366-377.
20. Law, R. W.; Margrave, J. L. Mass Spectrometer Appearance Potentials for Positive Ion Fragments from BF3, B(CH3)3, B(C2H5)3, B(OCH3)3, and HB(OCH3)2. *The Journal of Chemical Physics* **1956**, *25*, 1086-1087.
21. Noeth, H.; Staudigl, R.; Wagner, H. U. Contributions to the chemistry of boron. 121. Dicoordinate amidoboron cations. *Inorg. Chem.* **1982**, *21*, 706-716.
22. Higashi, J.; Eastman, A. D.; Parry, R. W. Synthesis and characterization of salts of the bis(diisopropylamido)boron(III) cation and attempted reactions to make the corresponding bis(dimethylamido)boron(III) cation. *Inorg. Chem.* **1982**, *21*, 716-720.
23. Hall, B. J.; Brodbelt, J. S. Comparison of cation binding affinities of quinones. *Int.l J. Mass Spectrom. Ion Processes* **1996**, *155*, 123-131.
24. Ranatunga, T. D.; Poutsma, J. C.; Squires, R. R.; Kenttamaa, H. I. The Heat of Formation of (Ch3o)2b+. *Int. J. Mass Spectrome. Ion Processes* **1993**, *128*, L1-L4.
25. Isbell, J. J.; Brodbelt, J. S. Use of borinium ions as probes of steric effects in gas-phase ion-molecule complexes. *Rapid Commun. Mass Spectrom.* **1996**, *10*, 1418-1420.
26. Ma, S. G.; Wong, P.; Cooks, R. G. Stereoelectronic effects and gas-phase affinities of dicoordinated borinium cations. *J. Mass Spectrom.* **1997**, *32*, 159-166.
27. Courtenay, S.; Walsh, D.; Hawkeswood, S.; Wei, P.; Das, A. K.; Stephan, D. W. Boron and aluminum complexes of sterically demanding phosphinimines and phosphinimides. *Inorg. Chem.* **2007**, *46*, 3623-31.
28. Srinivas, R.; Vivekananda, S.; Blanksby, S. J.; Schroder, D.; Schwarz, H.; Fell, L. M.; Terlouw, J. K. Generation and characterization of ionic and neutral dihydroxy boron B(OH)(2)(+/0) in the gas phase. *Int. J. Mass spectrom.* **2000**, *197*, 105-111.
29. Courtenay, S.; Mutus, J. Y.; Schurko, R. W.; Stephan, D. W. The extended borinium cation: [(tBu(3)PN)(2)B](+). *Angew. Chem. Int. Ed.* **2002**, *41*, 498-501.
30. Ranatunga, T. D.; Kenttamaa, H. I. Dicoordinated boron cations dehydrate organic ethers in the gas phase. *J. Am. Chem. Soc.* **1992**, *114*, 8600-8604.
31. Tanaka, N.; Shoji, Y.; Hashizume, D.; Sugimoto, M.; Fukushima, T. Formation of an Isolable Divinylborinium Ion through Twofold 1,2-Carboboration between a Diarylborinium Ion and Diphenylacetylene. *Angew. Chem. Int. Ed.* **2017**, *56*, 5312-5316.
32. Shoji, Y.; Tanaka, N.; Mikami, K.; Uchiyama, M.; Fukushima, T. A two-coordinate boron cation featuring C-B+-C bonding. *Nat. Chem.* **2014**, *6*, 498-503.
33. CFOUR, a quantum chemical program package written by J. F. Stanton, J. Gauss, M. E. Harding, P. G. Szalay, with contributions from A. A. Auer, R. J. Bartlett, U. Benedikt, C. Berger, D. E. Bernholdt, Y. J. Bomble, L. Cheng, O. Christiansen, M. Heckert, O. Heun, C. Huber, T. -C. Jagau, D. Jonsson, J. Juse´ lius, K. Klein, W. J. Lauderdale, D. A. Matthews, T. Metzroth, D. P. O'Neill, D. R. Price, E. Prochnow, K. Ruud, F. Schiffmann, W. Schwalbach, S. Stopkowicz, A. Tajti, J. Va´zquez, F. Wang, J. D. Watts, and the integral packages MOLECULE (J. Almlöf and P. R. Taylor), PROPS (P. R. Taylor), ABACUS (T. Helgaker, H. J. Aa. Jensen, P. Jørgensen, J. Olsen), and ECP routines by A. V. Mitin and C. vanWüllen, 2010.

34. Chai, J.-D.; Head-Gordon, M. Long-range corrected hybrid density functionals with damped atom-atom dispersion corrections. *Phys. Chem. Chem. Phys.* **2008**, *10*, 6615-6620.
35. Frisch, M.; Trucks, G.; Schlegel, H.; Scuseria, G.; Robb, M.; Cheeseman, J.; Scalmani, G.; Barone, V.; Mennucci, B.; Petersson, G. Gaussian 09, Revision B. 01; Wallingford, CT, 2009.
36. Weinhold, F.; Landis, C. R. *Discovering Chemistry with Natural Bond Orbitals* (Wiley, Hoboken NJ, 2012); Weinhold, F.; Landis, C. R.; Glendening, E. D. What is NBO analysis and how is it useful? *Int. Rev. Phys. Chem.* **2016**, *35*, 399-440; http://nbo6.chem.wisc.edu/.
37. (a) Bickelhaupt, F. M.; Baerends, E. J.The case for steric repulsion causing the staggered conformation of ethane. *Angew. Chem. Int. Ed.* **2003**, *42*, 4183−4188. (b) Weinhold, F. Rebuttal to the Bickelhaupt−Baerends case for steric repulsion causing the staggered conformation of ethane. *Angew. Chem., Int. Ed.* **2003**, *42*, 4188−4194.
38. Brunck, T. K.; Weinhold, F. Quantum-mechanical studies on the origin of barriers to internal rotation about single bonds. *J. Am. Chem. Soc.* **1979**, *101*, 1700−9; Reed, A. E.; Weinhold, F. Natural bond orbital analysis of internal rotation barriers and related phenomena. *Isr. J. Chem.* **1991**, *31*, 277−285; Goodman, L.; Pophristic, V.; Weinhold, F. Origin of methyl internal rotation barriers. *Acc. Chem. Res.* **1999**, *32*, 983−993.
39. Weinhold, F.; Landis, C. R. *Valency and Bonding: A Natural Bond Orbital Donor-Acceptor Perspective* (Cambridge U. Press, London, 2005).
40. Alabugin, I. V. *Stereoelectronic Effects: A Bridge between Structure and Reactivity* (Wiley, Hoboken NJ, 2016).
41. Weinhold, F. Chemical bonding as a superposition phenomenon. *J. Chem. Educ.* **1999**, *76,* 1141-1146; Ref. [36], p. 104, 123ff.
42. See, e.g., Cramer, C. J. Hyperconjugation as it affects conformational analysis. *J. Mol. Struct. (THEOCHEM)* **1996**, *370*, 135-146; Michl, J.; West, R. Conformations of linear chains. Systematics and suggestions for nomenclature. *Acc. Chem. Res.* **2000**, *33*, 821-823; Mikhailopulo, I. A.; Pricota, T. I.; Sivets, G. G.; Altona, C. 2'-chloro-2',3'-dideoxy-3'-fluoro-d-ribonucleosides: synthesis, stereospecificity, some chemical transformations, and conformational analysis. *J. Org. Chem.* **2003,** *68*, 5897-5908; Ribeiro, D. S.; Rittner, R. The role of hyperconjugation in the conformational analysis of methylcyclohexane and methylheterocyclohexanes. *J. Org. Chem.* **2003**, *68*, 6780-6787; Roberts, J. D. Fascination with the conformational analysis of succinic acid, as evaluated by NMR spectroscopy, and why. *Acc. Chem. Res.* **2006**, *39*, 889-896;
43. Schreiner, P. R. Teaching the right reasons: Lessons from the mistaken origin of the rotational barrier in ethane. *Angew. Chem. Int. Ed.* **2002**, *41*, 3579-3581; Carey, F. A.; Sundberg, R. J. *Advanced Organic Chemistry. Part A. Structure and Mechanisms*, 5th ed. (Springer, New York, 2007), p. 78ff; Dragojlovic, V. Conformational analysis of cycloalkanes. *ChemTexts* **2015**, *1*, 14.
44. Mo, Y.; Wu, W.; Song, L.; Lin, M.; Zhang, Q.; Gao, J. The magnitude of hyperconjugation in ethane: A perspective from ab initio valence bond theory. *Angew. Chem., Int. Ed.* **2004**, *43*, 1986−1990; Mo, Y.; Gao, J. Theoretical analysis of the rotational barrier of ethane. *Acc. Chem. Res.* **2007**, *40*, 113-119.
45. Ref. [39], p. 30-32.
46. Note that chlorine lone pairs also engage in strong n_{Cl}-p_B* hyperconjugation with the

adjacent p_B* orbital, sufficient to lead to default NBO depiction as a highly polarized 2-center π_{CCl}* valence antibond. For present purposes we employed $CHOOSE specification of the single-bonded σ_{BCl} Lewis-structural representation that insures retention of 1-center n_{Cl}, p_B* NBOs for consistent comparisons with other species.
47. Ref. [36], Sec. 5.3; *NBO Manual* (http://nbo.chem.wisc.edu/nbo6ab_man.pdf), p. B-23ff.
48. Badenhoop, J. K.; Weinhold, F. Natural bond orbital theory of steric interactions. *J. Chem. Phys.* **1997**, *107*, 5422-5432; Ref. [36], Sec. 6.1.

For Table of Contents Only

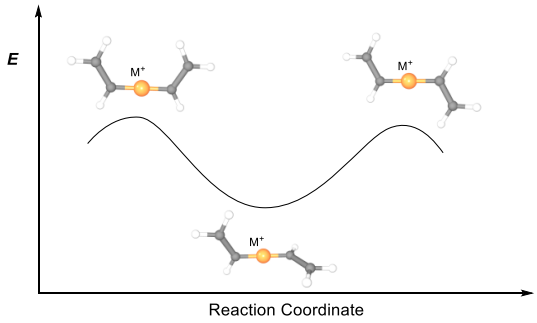

The divinylborinium cation and its heavier (Al, Ga, In, and Tl) congeners are studied, with unveiling the electronic origins of the torsional properties in terms of qualitative electronic structure concept.